LAWRENCE
LIVERMORE
NATIONAL
LABORATORY

LLNL-JRNL-655413

A high-resolution imaging X-ray crystal spectrometer for high energy density (HED) plasmas

H. Chen, M. Bitter, K. W. Hill, S. Kerr, E. Magee, S. R. Nagel, J. Park, M. B. Schneider, G. Stone, G. J. Williams, P. Beiersdorfer

June 4, 2014

Review of Scientific Instruments

Disclaimer

A high-resolution imaging X-ray crystal spectrometer for high energy density (HED) plasmas[a)]

Hui Chen[1], M. Bitter[2], K. W. Hill[2], S. Kerr[3], E. Magee[1], S. R. Nagel[1], J. Park[1], M. B. Schneider[1], G. Stone[1], G. J. Williams[1] and P. Beiersdorfer[1]

[1]*Lawrence Livermore National Laboratory, 7000 East Avenue, Livermore, California 94550-9234, USA*
[2]*Princeton Plasma Physics Laboratory, Princeton, New Jersey 08543, USA*
[3]*University of Alberta, Alberta T6G 2R3, Canada*

(Presented XXXXX; received XXXXX; accepted XXXXX; published online XXXXX)

Adapting a concept developed for magnetic confinement fusion experiments, an imaging crystal spectrometer has been designed and tested for HED plasmas. The instrument uses a spherically bent quartz [211] crystal with radius of curvature of 490.8 mm. The instrument was tested at the Titan laser at Lawrence Livermore National Laboratory by irradiating titanium slabs with laser intensities of 10^{19}-10^{20} W/cm^2. He-like and Li-like Ti lines were recorded, from which the spectrometer performance was evaluated. This spectrometer provides very high spectral resolving power (E/dE>7000) while acquiring a one-dimensional image of the source.

I. INTRODUCTION

Precision measurements of electron densities and ion temperatures through x-ray line broadening can provide critical information on plasma evolution and collisional equilibration processes. Better understanding of ion temperature equilibration in laser produced high energy density (HED) plasmas, including inertial confinement fusion implosions and short-pulse laser heated plasmas, is vital to improving the predictability of current simulation tools. Although plasma spectroscopy has long been used to diagnose the plasma temperature and density, the plasma conditions in HED plasmas are very different. For example, in a laser driven HED plasma, the plasma size is of sub-millimeter scale at near solid electron density. The electron temperatures are of keVs, and the plasma only lasts for a very short duration (pico- to nano-seconds). These conditions make it difficult to adopt the routine spectroscopy methods developed for other types of plasmas, such as magnetically confined fusion plasmas. In this paper, we describe the design and test of a high-resolution crystal spectrometer using a spherical crystal with one-dimensional imaging of the source size. Similar crystal designs have been developed for large Tokamak plasmas and laser experiments[1-4] and ref. cited therein]. This particular technique is now being adapted for HED plasmas produced by high intensity lasers.

II. SPECTROMETER DESIGN

The spectrometer was designed for the observation of He-like titanium in the wavelength range from 2.55 Å to 2.65 Å with use of a spherically bent quartz-2131 crystal, which had a 2d-lattice spacing of 3.07960 Å and a radius of curvature R = 490.8 mm. The width and height of the crystal were 50 mm and 30 mm, respectively. A schematic of the experimental arrangement is shown in Fig. 1. The x-ray source, crystal, and detector were centered at the points A, C, and B, respectively. Also shown is a Rowland circle of diameter R, which passes through the center of the crystal sphere, at the point O, and the center of the crystal surface, at the point C. This circle intersects the extension of the straight line A-O at B. Photons, emitted from a point source at A, strike the crystal surface at different points with different angles of incidence and are Bragg reflected if the Bragg condition is fulfilled. Shown in Fig. 1, are the incident and reflected rays for the central point C and two edge points on the crystal surface. Since the crystal is a sphere, the ray pattern is symmetric with respect to rotations about the axis A-O-B and, in general, with respect to rotations about any axis which passes through the center O of the crystal sphere. The intersection points of the reflected rays with the axis A-O-B are fixed points with respect to rotations of the ray pattern about this axis and represent the images of a point source at A for different wavelengths λ that are formed by the sagittal rays. Our experimental arrangement was such that the resonance line w with the wavelength of 2.6097 Å was reflected from the point C at the center of the crystal surface and focused to the point B on the Rowland circle. The distances O-A, O-B, C-A, and C-B were, therefore, equal to O-A = -Rcos(Θ_w)/cos(2Θ_w) = 597 mm, O-B = Rcos(Θ_w) = 260.6 mm, C-A = -Rsin(Θ_w)/cos(2Θ_w) = 953.4 mm, and C-B = R sin(Θ_w) = 415.9 mm, since the Bragg angle for w-line was Θ_w = 57.93°. The observable wavelength range was: 2.56 $\leq$ λ $\leq$ 2.66 Å, since

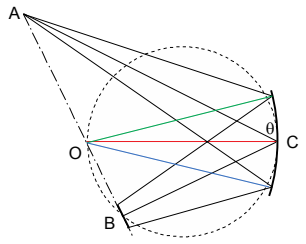

FIG. 1: The principle of the imaging crystal spectrometer.

[a)]Contributed (or Invited) paper published as part of the Proceedings of the 20th Topical Conference on High-Temperature Plasma Diagnostics, Atlanta, Georgia, June, 2014.
[b)]Author to whom correspondence should be addressed: chen33@llnl.gov

the width of the crystal in the main dispersion plane (drawing plane of Fig. 1) was 50 mm. The spectrometer also provided images of the plasma source at A with a one-dimensional spatial resolution in a direction perpendicular to the main dispersion plane, since the ray pattern was also symmetric with respect to rotations about an axis in the drawing plane of Fig. 1 that passes through O and is perpendicular to the axis A-O-B. The magnification M of this 1D imaging is equal to M = O-B/O-A = -cos(2Θ_w) = 0.436.

The theoretical resolving power as determined from the angular width of the crystal rocking curve for a flat quartz-2131 crystal is 75000. However, the resolving power of a bent crystal can be smaller due to the fact that the shape and width of the rocking curve also depend on the curvature of the crystal lattice.[1,5] A preliminary off-line measurement of the rocking curve of the spherically bent crystal, which was used in our experiments, showed that the FWHM reflectivity width was less than 190 μrad at the wavelength of the Ti Kα1 line, which gives a lower limit for the resolving power of $\lambda/\Delta\lambda$=5000 at this wavelength.[6] As discussed below, an upper limit of about 7300 for the achievable resolving power was set in our experiment by source size broadening.

To use the spectrometer in the environment of an intense laser (with intensity > 10^{16} W/cm^2), we need to consider the high radiation background from fast particles (electrons, protons and ions) and the scattering processes which produced high-energy (up to MeV) photons. We designed a light-tight housing (Fig. 2) made of aluminum plate, which was chosen for its low scattering cross-section. Heavier materials were added outside the Al house for additional shielding: a 25 mm thick high-Z collimator was placed in front of the crystal and 25 mm thick lead surrounded the detector. We chose to use image plates as well as x-ray film as the detector rather than the CCD detectors used elsewhere[2-4] to avoid the impact of electromagnetic pulses to the electronics. For the alignment, a fixed pointer was installed in front of the spectrometer housing. After the alignment, it is removed for shots. A light-tight aluminized mylar window separated the spectrometer and the source.

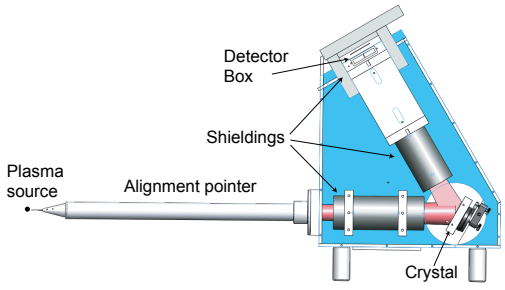

FIG. 2: The cross-section of the spectrometer.

III. EXPERIMENT ON TITAN LASER

The imaging crystal spectrometer was tested on the Titan laser at the Jupiter Laser Facility in Lawrence Livermore National Laboratory. The 1054 nm laser has a pulse length of 700 fs. The laser energy was about 100 J. Focused by an off-axis parabola, the spot size on target was about 10 micron in full-width at half-maximum. The peak laser intensity was between 8x10^{19} and 5x10^{20} W/cm^2. The targets were Ti foils (260 um in thickness and 6.5 mm in diameter). The intense laser field and collisions rapidly heat and ionize the target to produce a hot plasma with ions stripped down to their K shell. There are steep temperature and density gradients in this hot plasma. Hydrodynamic simulation shows that the electron density varies from solid (10^{23} cm^{-3}) at the target surface to about 10^{20} cm^{-3} a few hundred microns away. The temperature ranges from a few tens of eV near the solid to a few keV in the plasma plume [7]. It is through such gradients that the Ti K-shell emission was observed.

A sample of a Ti spectrum collected by the spectrometer is shown in Fig. 3. The main spectral features have been identified as the main He-like lines w, x, and y and the associated Li-like

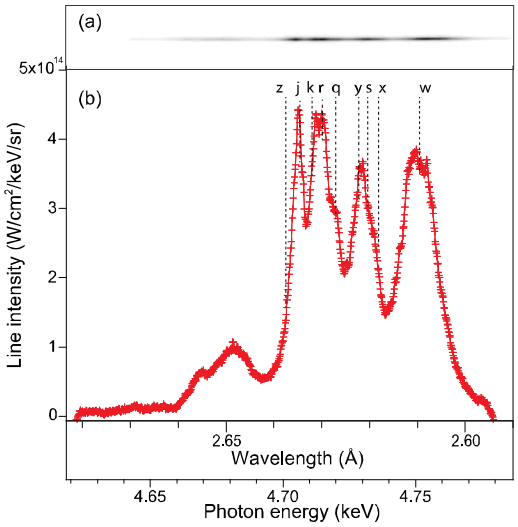

FIG. 3: The raw data image (a) and the lineout (b) of the spectrum from a Ti target. The line intensity is estimated using the spectrometer collection efficiency and image plate response.

n=2 satellites of Ti – see Table 1. From a comparison with the He-like Ti spectra from TFTR tokamak plasmas[8], we conclude that the features of the spectrum shown in Fig. 3 are significantly broadened by opacity broadening and possibly Stark broadening. We also note that the forbidden line z, which is often used for density measurements, is absent in the Ti spectrum, shown in Fig. 3, and that it is a very prominent feature in the spectra from TFTR tokamak plasmas – see Fig. 4 in ref. 8. The absence of the line z indicates that the plasma density was so high that the 2s level was depopulated by ion and electron collisions rather than by radiative 2s-1s transitions. The theoretically predicted rate for these radiative 2s-1s transitions in He-like Ti is 3.76x10^7 s^{-1} – see ref. 10. Another observation is that the dielectronic satellite **j** is a prominent spectral feature that is not opacity broadened. This is due to the fact that the doubly-excited upper state for this satellite line– see Table 1 - can only be produced by resonant electron capture and **not** by photoexcitation or the absorption of a photon, which is the cause for opacity broadening. The satellite j should, therefore, be well suited for ion-temperature or Stark broadening measurements.

It was found that the spectrometer housing was well designed because the signal to noise ratio in the measured spectrum was greater than 10 across the spectral range. This is likely due to the combination of reduced background noise from

hard x rays and energetic particles via shielding materials and the high collection efficiency of the spherical crystal geometry.

The recorded Ti spectral features and the associated charge states, listed in Table 1, were identified using the atomic code FLYCHK[9] and Ref. 8. As already mentioned, the opacity effect was significant for the He-like resonance line (w) and inter-combination lines (x, y). We found that FLYCHK calculations for a 50 micron deep plasma with a 2 keV plasma temperature at $5x10^{22}$ cm^{-3} electron density provided the best fit to the observed line features. The calculation was for steady state, non-LTE plasmas and did not capture the line width from the range of temperature and density range. Detailed spectral analysis will require a spectral model coupled to a dynamic plasma evolution model that will be performed in the future.

Table 1. Theoretically predicted wavelengths for the main spectral features in the spectrum of He-like Ti, taken from ref. 8.

Symbol	Wavelength (Å)	Transition
w	2.6097	$1s^2\ ^1S_0 - 1s2p\ ^1P_1$
x	2.6184	$1s^2\ ^1S_0 - 1s2p\ ^3P_2$
s	2.6205	$1s^22s\ ^2S_{1/2} - 1s2s2p\ ^2P_{3/2}$
y	2.6223	$1s^2\ ^1S_0 - 1s2p\ ^3P_1$
q	2.6273	$1s^22s\ ^2S_{1/2} - 1s1s2p\ ^2P_{3/2}$
r	2.6295	$1s^22s\ ^2S_{1/2} - 1s1s2p\ ^2P_{1/2}$
k	2.6313	$1s^22p\ ^2P_{1/2} - 1s2p^2\ ^2D_{3/2}$
j	2.6348	$1s^22p\ ^2P_{3/2} - 1s2p^2\ ^2D_{5/2}$
z	2.6362	$1s^2\ ^1S_0 - 1s2s\ ^3S_1$

The imaging property of the spectrometer was found to be limited by the resolution of the detector. The minimum spatial resolving size for an image plate is about 70 microns[10], and is about 20 microns for x-ray film. The magnification of the spectrometer is about 0.44. For a source size of about 50 microns, the image is less than the tested resolving power of the detector. Figure 4 shows the lineout along the imaging direction for an x-ray film. This lineout is about 3 pixels full-width half maximum, yielding a deconvolved source size of about 100 microns, which is larger than that determined by an x-ray pinhole camera fielded in the experiment. Although it is possible that the crystal was not in the best focal position, the detector's spatial resolution also prohibited the measurement of source sizes that were smaller than 20 microns. To make use of the imaging capability using these film-based detectors, a larger magnification setup is needed, as the detector resolution used in this experiment is approaching the limit of presently available technology. Although the plasma source size was only measured in the direction perpendicular to the main dispersion plane, it is reasonable to assume that the source size in the main dispersion plane was of the same magnitude. With this assumption, we calculated the effect of source broadening and obtained the above-mentioned upper limit of $\lambda/\Delta\lambda$=7300 for the achievable spectral resolving power.

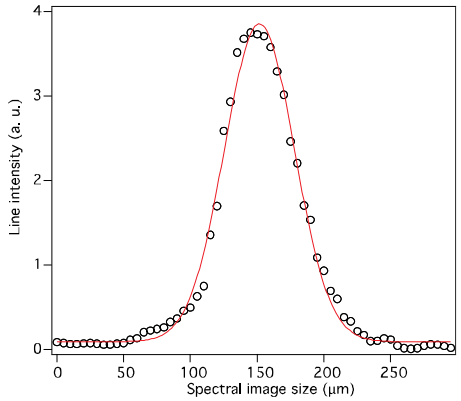

FIG. 4. The lineout along the imaging direction of the spectrum. The detector used was x-ray film, scanned at 15 micron resolution.

VI. SUMMARY

The spherical crystal spectrometer has been successfully tested on a laser-produced HED plasma. The spectrometer has three main advantages: high spectral resolving power, high collection efficiency and one-dimensional imaging capability. Proper shielding allows it to be fielded in the high noise environment of high-energy laser experiments. Coupled to dynamic modeling, the time-integrated spectrum from such a spectrometer can provide information on the plasma temperature, density, and emission size. Coupled to an appropriate streak camera or framing camera, the spectral (and possibly the source size information, if resolved) can be directly compared to a model to provide valuable benchmark information. It is fully expected that such an instrument will be fielded in various large laser facilities in the near future[11]. Since a precise knowledge of the spectrometer's resolving power will be needed for spectral line-shape measurements, we intend to determine this important parameter from additional tests of the spectrometer with a micro-focus x-ray tube and by performing experiments at an electron-beam ion trap.

This work was performed under the auspices of the U.S. DOE by LLNL under Contract DE-AC52-07NA27344 and was supported at PPPL under DOE contract DE-AC02-09CH11466.

V. REFERENCES

[1]M. Bitter, *et al.*, Rev. Sci. Instrum. **70**, 292 (1999); B. S. Fraenkel, M. Bitter, S. von Goeler and K. Hill, *J. X-ray Sci. Technology*, **7**, 171 (1997)
[2]A. Ince-Cushman, J. E. Rice, M. Bitter, M. L. Reinke, K. W. Hill *et al.*, *Rev. Sci. Instrum.* **79**, 10E302 (2008).
[3]K. W. Hill, M. L. Bitter, S. D. Scott, A. Ince-Cushman, M. Reinke *et al.*, *Rev. Sci. Instrum.* **79**, 10E320 (2008); K. W. Hill, M. Bitter, L. Delgado-Aparicio, *et al.*, *Rev. Sci. Instrum.* **81**, 10E322 (2010).
[4]L M Belyaev, A B Gil'varg, Yu A Mikhaĭlov, *et al.*, Soviet Journal of Quantum Electonics, 7, 67, (1977); S. A. Pikuz, T. A. Shelkovenko and V. M. Romanova *et al.*, *Rev. Sci. Instrum.* **68**, 740 (1997).
[5]I. Uschmann, E. Förster, K. Gäbel,G. Hölzer, M. Ensslen, J. Appl. Cryst. **26** 405 (1993); P. Beiersdorfer, S. von Goeler, M. Bitter, K. W. Hill, R. A. Hulse and R. S. Walling, *Rev. Sci. Instrum.* **60**, 895 (1989); E. Wang, P. Beiersdorfer, M. Bitter, *et al.*, *Rev. Sci. Instrum.* **81**, 10E329 (2010).
[6]M. Haugh, *private discussion* (2014)
[7]W. Theobald, K. Akli, R.Clarke, et al., *Phys. Plasmas* **13**, 043102 (2006)
[8]M. Bitter, K. W. Hill, M. Zarnstorff, et al., *Phys. Rev. A*, **32**, 3011 (1985)
[9] H. K. Chung, *High Energy Density Physics* **1**, 3 (2005)
[10]B. R. Maddox, H.-S. Park, B. A. Remington, N. Izumi, S. Chen, C. Chen, G. Kimminau, Z. Ali, M. J. Haugh, and Q. Ma, *Rev. Sci. Instrum.* **82**, 023111 (2011).
[11]M. Bitter, K. W. Hill, N. A. Pablant, L. F. Delgado-Aparico, P. Beiersdorfer, J. Dunn, M. Sanchez del Rio, LLNL-PROC-490512